Multiaxial fatigue behaviour of hot-rolled crane runway beams with welded block rail

Ulrike Kuhlmann[a], Mathias Euler[a]

[a] Institute for Structural Design
Universitaet Stuttgart, 70569 Stuttgart, Germany

Abstract Top running overhead cranes belong to the important equipment of modern production halls. Mostly, crane runway beams form the crane supporting structure. Usually, a crane runway beam consists of a hot-rolled I-section with a block rail fixed to the top flange by rail welds (fillet welds). The current fatigue design of crane runway beams according to Eurocode 3 Part 1-9 uses the Classification method (*S-N* method). This approach does not consider the complex multiaxial state of stress in the vicinity of the rail welds to its entire extent. At the point of wheel load application the top region of a crane runway beam is subjected to longitudinal stresses σ_x due to bending in addition to local stresses resulting from the load application. The fatigue verification has to account for all applied stresses what makes it quite complex. On the other hand simplifications are used that tend to underestimate the fatigue resistance. The goal of the still ongoing research is to analyse the influence of the wheel load application on the fatigue resistance of the longitudinal fillet weld, a structural detail specified in Eurocode 3 Part 1-9. Therefore a test program was set up comprising eight test girders and several small scale specimens that simulated a multiaxial cyclic loading. Different types of frequently used rail welds (such as continuous and intermittent ones) were investigated. This paper presents the test results.

1 INTRODUCTION

The vast majority of crane runway beams for top running overhead cranes are made of steel (Fig. 1*a*). Approximately 70 % of all crane runway beams are designed for light and moderate crane service and usually consist of a hot-rolled section with a block rail fastened to the top flange by automatic fillet welds.

The fatigue verification of a crane runway beam according to Eurocode [7] is based on the *S-N* method. In general the verification is mainly focused on the rail welds. Although the *S-N* method is already a simplification the verification is still complex because of the variety of stress ranges that have to be taken into account.

At the point of wheel load application the top region of the crane runway beam is subjected to a multiaxial, non-uniform state of stress. This state of stress comprises local stresses caused by the load application in addition to longitudinal stresses σ_x due to bending (see Fig. 1*b*). The application of the concentrated wheel load leads to local transverse compressive stress σ_z and local shear stress τ_{xz}. Differently to the uni-directional local stress σ_z the bending stress may be either positive or negative depending on the structural system of the crane runway beam.

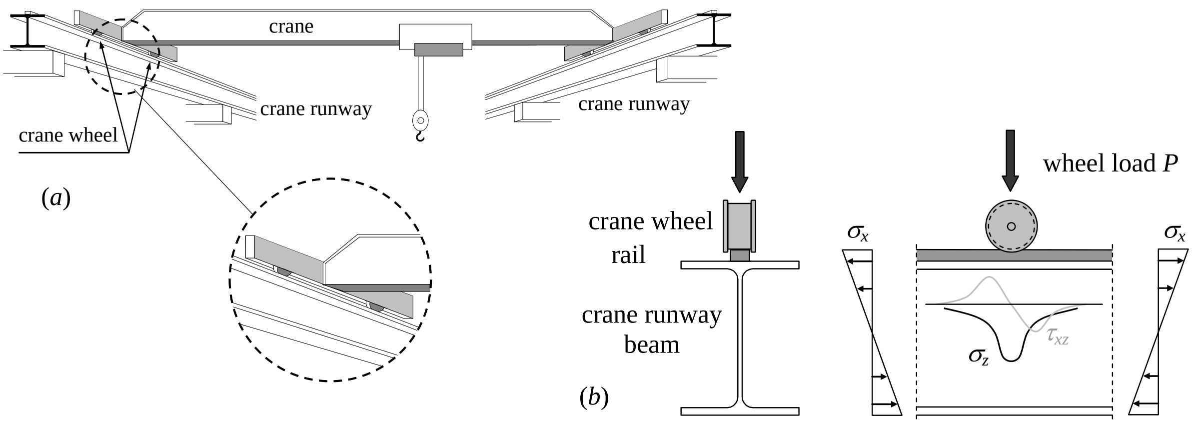

Figure 1. (*a*) Top running overhead crane, (*b*) wheel load application

Since crane loads are cyclic loads each crane passage results in a number of loading cycles with definite stress ranges of each stress component. Hereby the number of cycles of the different stress components can vary since one pass of the crane may result in more than one loading cycle depending on the number of crane wheels on the rail and the pitch of the wheels. Thus the number of loading cycles of the local stress ranges is usually greater than that of bending stress because of the more numerous wheel passages. That is why that this kind of dynamic loading is called combined multiaxial, non-proportional cyclic stressing.

2 QUESTIONS TO SOLVE

2.1 Present specifications of Eurocode [7]

From the viewpoint of fatigue all stress ranges have to be accounted for. Each single stress component has to be verified. Furthermore the cumulative effect of the combined action, which means the multiaxial state of stress, has to be determined using the Palmgren-Miner rule, see equation (1).

$$\left(\frac{\gamma_{Ff}\cdot\Delta\sigma_{E,x}}{\Delta\sigma_{C,x}/\gamma_{Mf}}\right)^3+\sum_n\left(\frac{\gamma_{Ff}\cdot\Delta\sigma_{E,z}}{\Delta\sigma_{C,z}/\gamma_{Mf}}\right)^3+\sum_n\left(\frac{\gamma_{Ff}\cdot\Delta\tau_{E,xz}}{\Delta\tau_{C,xz}/\gamma_{Mf}}\right)^5\leq 1 \qquad (1)$$

with n … number of wheel passages per crane passage

The structural detail of the rail weld has to be categorized in order to determine its fatigue resistance. Because of the various stress components the rail weld has to be classified for each stress component separately.

The rail weld in tension or compression σ_x corresponds closely to the detail of the automatic longitudinal fillet weld with start-stop positions specified in [7]. The appropriate category is 112. The rail weld subjected to local shear stress can be compared with the shear flow transmitting continuous fillet weld specified in [7]. Hence it is classified as category 80. The rail weld being stressed by local transverse pressure σ_z is not explicitly defined in [7]. Normally, the similar detail of the top flange to web junction is used to assess the rail weld [6] (see Fig. 2*a*). Thus the rail welds fall into the lowest category 36, available in Eurocode.

The low classification of the top flange to web junction goes back to the early 1960s. At that time the allowable fatigue stress range was not determined by tests, but the corresponding fatigue resistance was derived by comparison. The compressive stress transmitting top flange to web junction was considered to behave like a cruciform joint in tension in terms of fatigue (see Fig. 2*b*). The influence of the favourable mean compressive stress was accounted for by higher fatigue strengths [8]. According to the philosophy of the Eurocode the fatigue resistance of a welded steel structure is either hardly or not at all affected by the mean stress. As a consequence both details, the top flange to web junction in compression and the cruciform joint in tension, have been classified as the same quite low fatigue category 36. Subsequently, this also holds for the rail welds.

Since both details covering the local stress components do not allow for the stress concentration due to the wheel load application, modified nominal stresses have to be used to make the check.

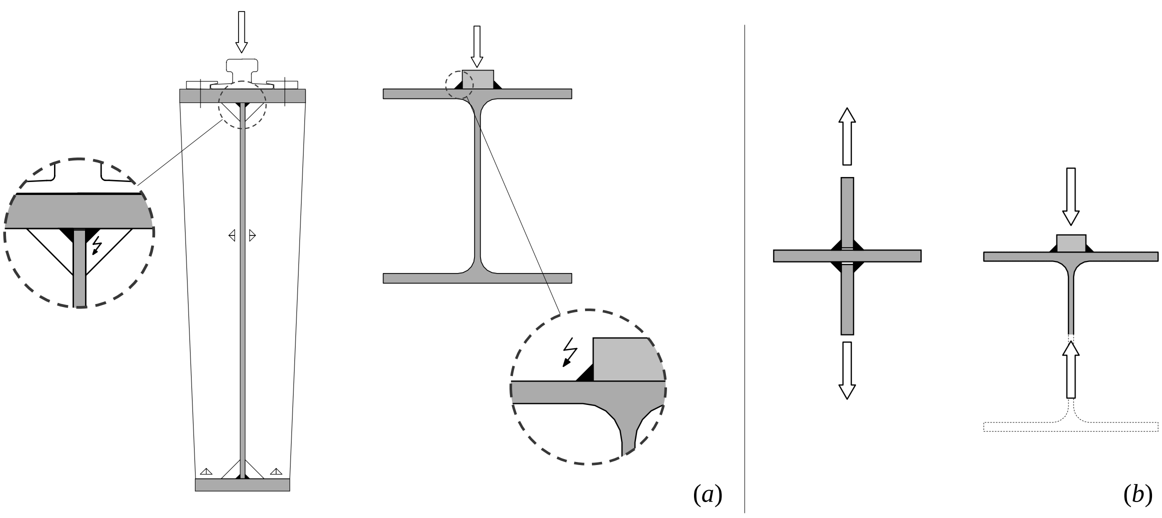

Figure 2. Comparable structural details: (*a*) top flange to web junction in case of light crane service, (*b*) cruciform joint

2.2 Existing test data

In the 1960-70s efforts were made to establish experimentally based fatigue strengths of the top flange to web junction under wheel load application. Among the available test data in literature the publications of *Gurney* [4, 5] and *Dittrich* & *Ernst* [1] are especially to be mentioned.

Gurney investigated the fatigue behaviour of small scale T-specimens cut from rolled and welded beams under cyclic wheel loads (uniaxial stress). The influence of longitudinal stresses and the influencing effect of the rail weld were neglected.

In the 1970s *Dittrich* & *Ernst* tested crane runway beams with welded section under multiaxial stressing. In four-point bend tests single-span runway beams with various top flange to web junctions were tested. Thus the welds under consideration were subjected to longitudinal and transverse compressive stress. In none of the tests fatigue failure has been recorded.

2.3 Tests on small scale specimens and planning of girder tests

At the beginning of the research project small scale T-specimens cut from hot-rolled beams with welded block rail were tested under cyclic loads with constant amplitude. The influence of a pulsating compressive single load (wheel load) as well as the influence of a pulsating tensile and an alternating single load were investigated. As expected the rail welds under alternating or pulsating tension loading failed through weld cracking from the weld root. On the contrary no fatigue failure occurred under pulsating compression loading.

With respect to these test results and the available test data from literature it seemed to be not promising to test single-span test girders. In case of a single-span girder the local transverse compressive stress is superposed by the longitudinal compressive stress due to bending in the top region. The resulting state of stress can be considered favourable with respect to the maximum-distortion-energy theory. Therefore it was deemed to investigate a pulsating wheel load in combination with longitudinal tensile stresses (Fig. 3*c*). This state of stress is typical of multiple-span crane runway beams (Fig. 3*a*, 3*b*).

The allowable fatigue stress range of longitudinal fillet welds in tension is well-known by an extensive data-base. The intention of the planned girder tests should therefore be to show whether and how this fatigue strength decreases through the application of an additional wheel load. That means that the damage contribution of the wheel load would be determined indirectly (see Fig. 3*d* and [2]).

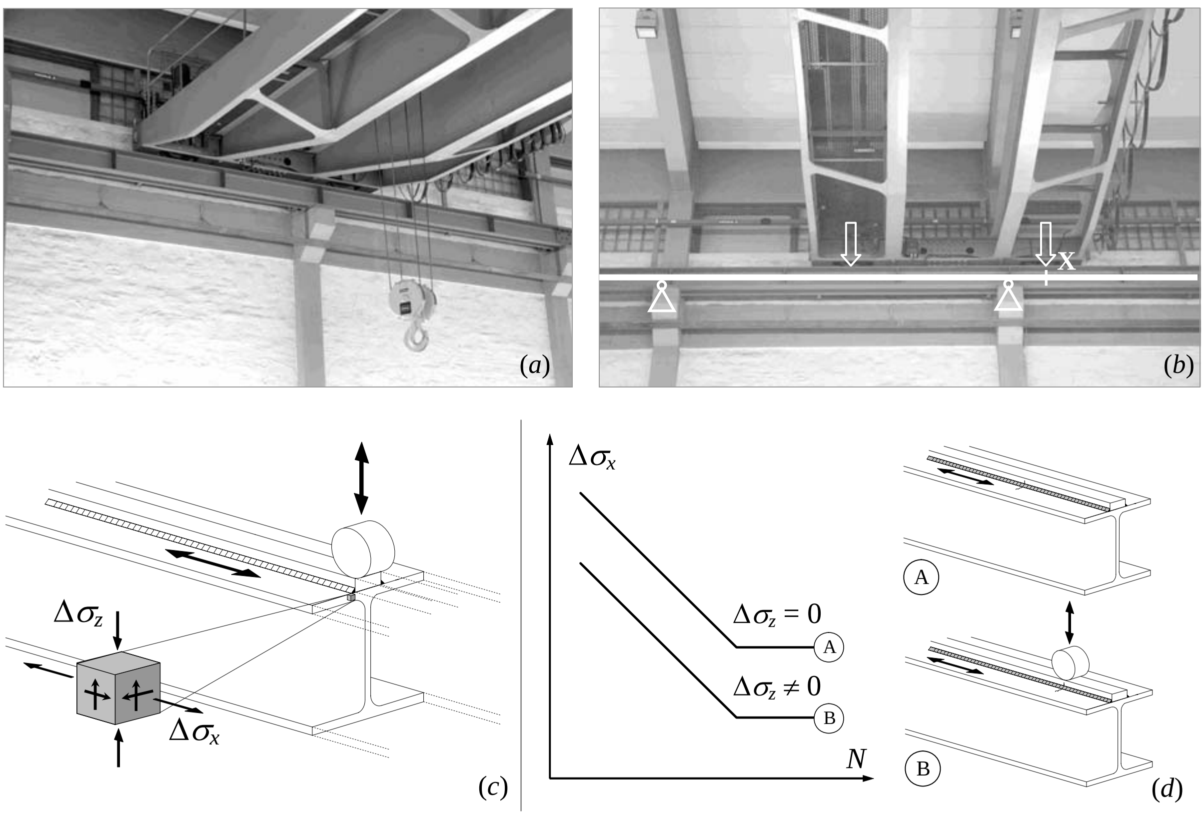

Figure 3. (*a*), (*b*) Realized multiple-span crane runway, (*c*) stress field at position X, (*d*) schematic diagram of indirect wheel load's influence on the fatigue strength of longitudinal fillet welds in tension

3 TESTS ON CRANE RUNWAY BEAMS

The test setup shown in Fig. 4 was chosen to simulate the multiaxial cyclic stressing. The test girders were subjected to pulsating compressive forces at the locations *a*, *c* and *e* by means of two synchronously working hydraulic jacks and two traverse beams. Thus the bending moment between the locations *b* and *d* has been nearly constant. The range of the flexural tensile stress σ_x at the top flange's upper surface amounted to 144 N/mm² with a stress ratio $R \approx 0$. The wheel load at midspan was introduced by a pressure stamp simulating a crane wheel ∅ 200 mm. The maximum wheel load measured $P_1 \approx 160$ kN, the minimum load was about 3 kN. The test frequency was between 2 to 3 Hertz.

The test girders had a hot-rolled section (HE 400 A) of steel grade S 235 with welded block rail 50 x 30 mm of steel grade S 355. There were three girders with continuous rail welds of a = 4 mm (Type A in Figure 5*a*), two with chain intermittent fillet welds of a = 5 mm (L = 60 mm) and a spacing of s = 300 mm (Type B) and two with staggered intermittent fillet welds of a = 5 mm (L = 100 mm) and a spacing of s = 700 mm (Type C). Additionally, a reference test with continuous fillet welds without wheel load was carried out.

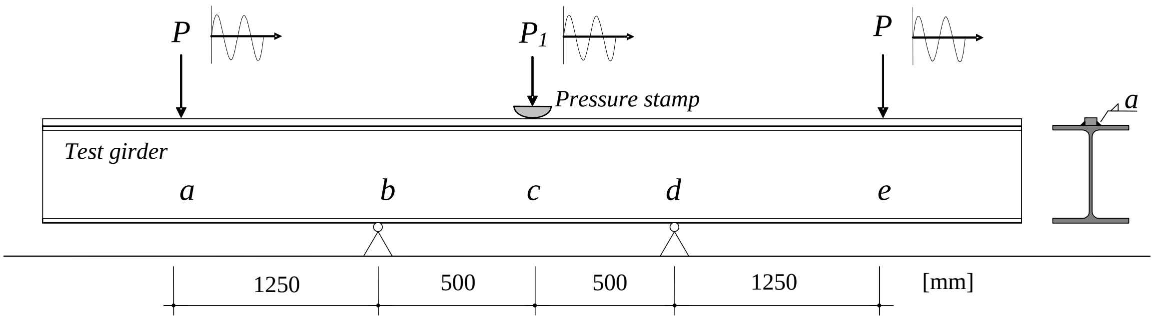

Figure 4. Test setup

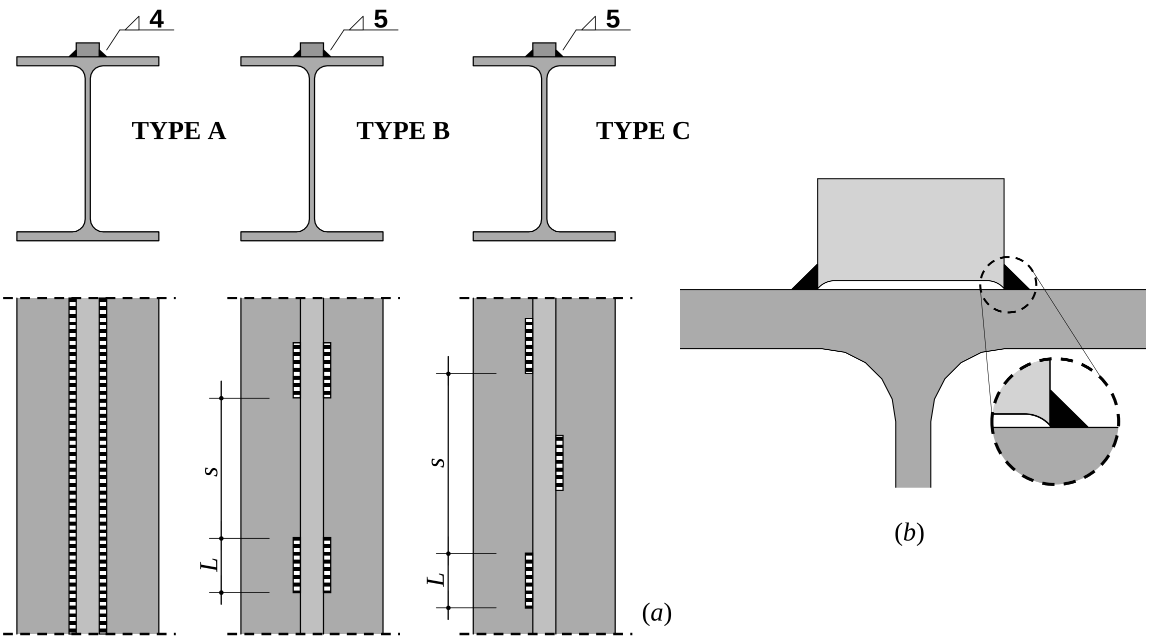

Figure 5. (*a*) Tested types of rail welds, (*b*) recessed rail bottom

The bottom rail surface was recessed in the way shown in Fig. 5*b*. The recess should ensure that the load transfer from the rail to the top flange was exclusively realized by the rail welds. Hence all loads acting on the top surface of the rail were transmitted into the top flange by the rail welds. By avoiding the top flange to rail contact the rail welds were stressed most. In reality such a situation may be caused by the shrinkage of the top flange during cool-down of the rail welds after welding. Also the hollow between rail and top flange may result from an inappropriate fixation while placing the rail welds. The hollow stays normally undetected since no visual check is possible. In case of intermittent fillet welds this problem does not occur because of the possible visual check and the far less heat-up of the top flange during the welding. The surface of the milled-out portion at the rail bottom was left rough in order to create a surface with the same notch effect like the millscale surface.

4 TEST RESULTS

4.1 Continuous rail welds

The failure mode (Fig. 6*a*, *b*) and the observed crack growth (Fig. 6*c*) of the tests on continuous rail welds are shown in Fig. 6. The visible crack is referred to as primary crack. At the end of the tests the beams were cut and the fracture surfaces were examined. The microscopic examination and the test-related observations suggest a fracture mechanism comprising three phases.

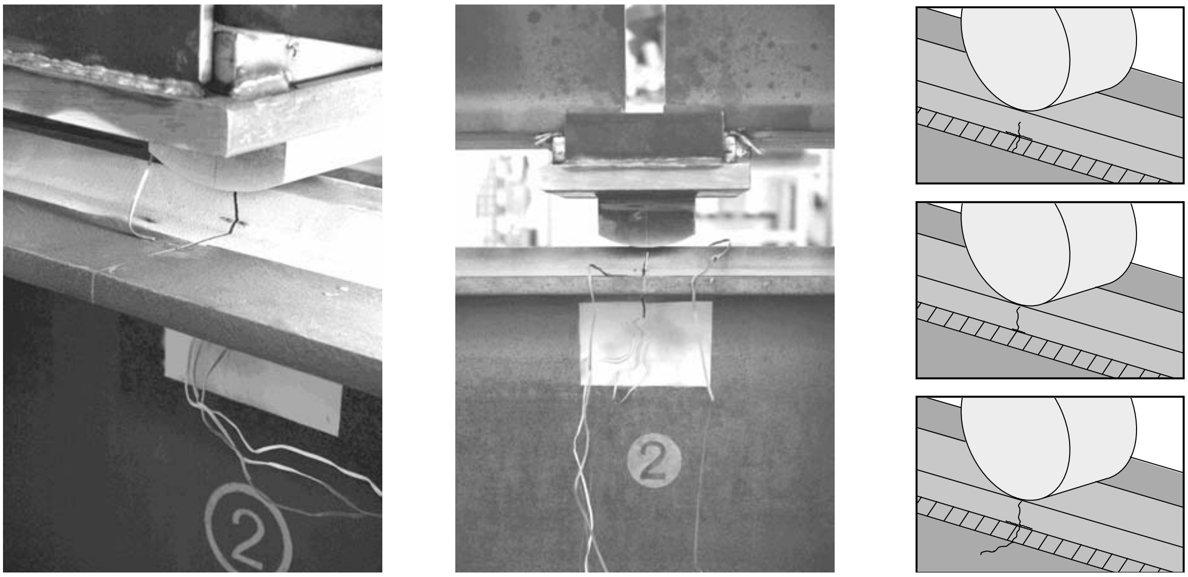

(*a*) (*b*) (*c*)

Figure 6. (*a*), (*b*) Failure of continuous rail weld beneath the stamp in midspan, (*c*) observed crack growth

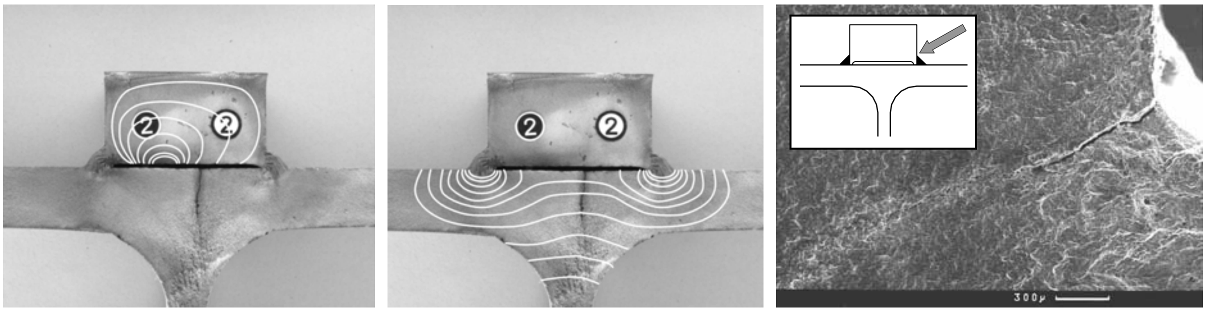

Figure 7. Fracture surface: (*a*) phase 1, (*b*) phase 3 of primary crack's propagation; (*c*) secondary crack at the weld toe

The primary crack was initiated at the bottom surface of the rail right below the wheel load (phase 1, see fig. 7*a*). After the rail through-crack the rail welds failed in a ductile manner (phase 2). Subsequently, the crack propagated into the top flange leading to two crack growth centres (phase 3, see Fig. 7*b*). Presumedly during phase 2, secondary cracks to each side of the rail developed right beneath the wheel load from the weld toes, see Fig. 7*c*. These cracks were hardly detectable from outside. Their fracture plane was oriented normal to that of the primary crack.

In the following the fatigue effect of the investigated continuous rail welds is compared to the longitudinal fillet welds without wheel load to identify the damage contribution of the wheel load. In Fig. 8 the test results of this research project are plotted together with the scatter band of a test series on longitudinal welds (Identification code 3_2_WBS 5 in [9]). The test series on longitudinal fillet welds has a characteristic fatigue strength $\Delta\sigma_C$ = 114.5 N/mm² (95% survival with 75% confidence). Thus it quite well represents the fatigue category 112. The results of the own test girders with continuous rail welds lie near the lower bound of the scatter band. It turned out that the wheel load significantly contributed to the fatigue damage. Since the fatigue failure occurred directly beneath the wheel load a damage contribution of the local shear stress can be excluded (see Fig. 1*b*).

A three-dimensional FE analysis in [3] revealed that the missing contact between rail and top flange leads to a local stress peak σ_x at the bottom surface of the rail. The present approach of [6] dealing with the load application just considers the local stress concentrations of σ_z and τ_{xz} and neglects any influence of the wheel load application on the longitudinal stress σ_x. This seems to be non-conservative looking at the recorded failure mode.

The reference test on continuous rail welds without wheel load survived more than 4,5 million cycles lacking any onset of failure of the top flange (run-out ↗, see Fig. 8). So it lies close to the upper bound of the scatter band for tests on longitudinal fillet welds. This result is so far important since it shows that the recess at the rail bottom did not affect the fatigue strength. Furthermore this outcome corresponds well with the experience that current fatigue tests lead to higher fatigue resistances than those measured in 1970s because of the meanwhile improved welding and material processing. This is especially true for automatically welded structural details.

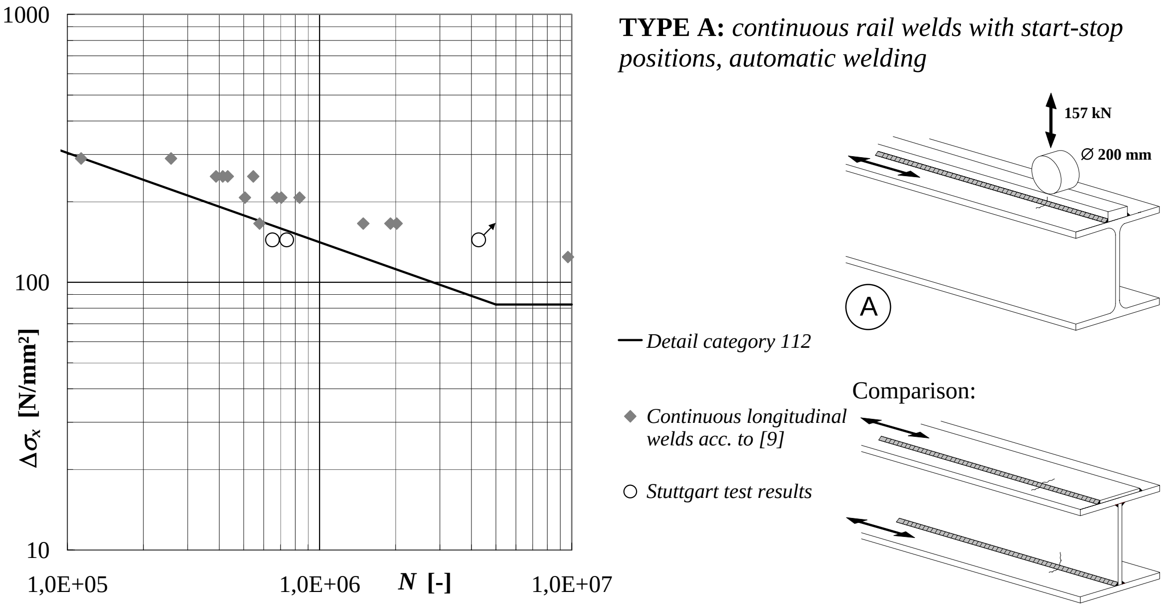

Figure 8. Fatigue strength of continuous rail welds

4.2 Intermittent rail welds

The fracture mechanism of intermittent rail welds being visible from outside differed from that of the continuous rail welds. Simultaneously, many cracks were initiated at the weld ends regardless of the position of wheel loading, see Fig. 9. One of these cracks led to the through-crack of the rail. Afterwards crack growth into the top flange accelerated starting from a weld end adjacent to the rail through-crack. The fracture of the rail welds subjected to wheel loading was recorded in two tests.

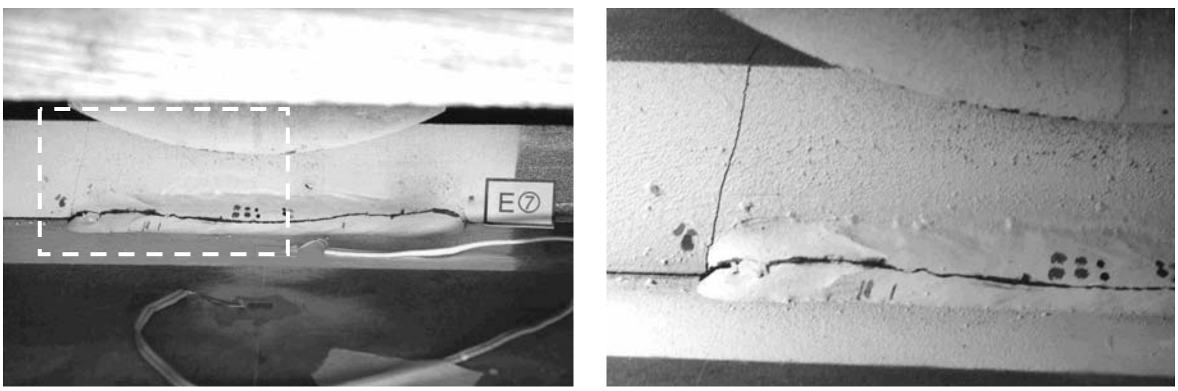

Figure 9. Failure mode of staggered intermittent rail welds with wheel loading, detail (right)

In the following the fatigue effect of the chain intermittent and staggered intermittent welds are compared to the structural detail of the (unloaded) longitudinal stiffener with a length of $50 < L \leq 80$ mm respectively $80 < L \leq 100$ mm. According to Eurocode this detail falls into the fatigue category 71 respectively 63. A comparison with the intermittent longitudinal fillet welds (category 80) is not possible since the ratio of weld length and spacing is outside the defined scope. In Fig. 10 and 11 the own test results are plotted together with the scatter band of a test series on longitudinal stiffener with L > 100 mm (Identification code 1_1_p acc. to. [9]). Unfortunately, there are no test results on 60 mm longitudinal stiffeners available. The fatigue strength of the considered test series on longitudinal stiffeners amounts to $\Delta\sigma_C$ = 76.5 N/mm². Thus it is representative of fatigue category 71 although the detail belongs to category 63 according to Eurocode. The own test results fit well into the scatter band. All test results of chain intermittent rail welds lie above the *S-N* curve 71, and only one test result of the staggered intermittent rail welds (without wheel load) is positioned beneath the *S-N* curve 63.

It can be concluded that the fatigue behaviour of the intermittent rail welds is predominantly controlled by the high notch effect of weld ends rather than the stress-rising effect of the wheel load application.

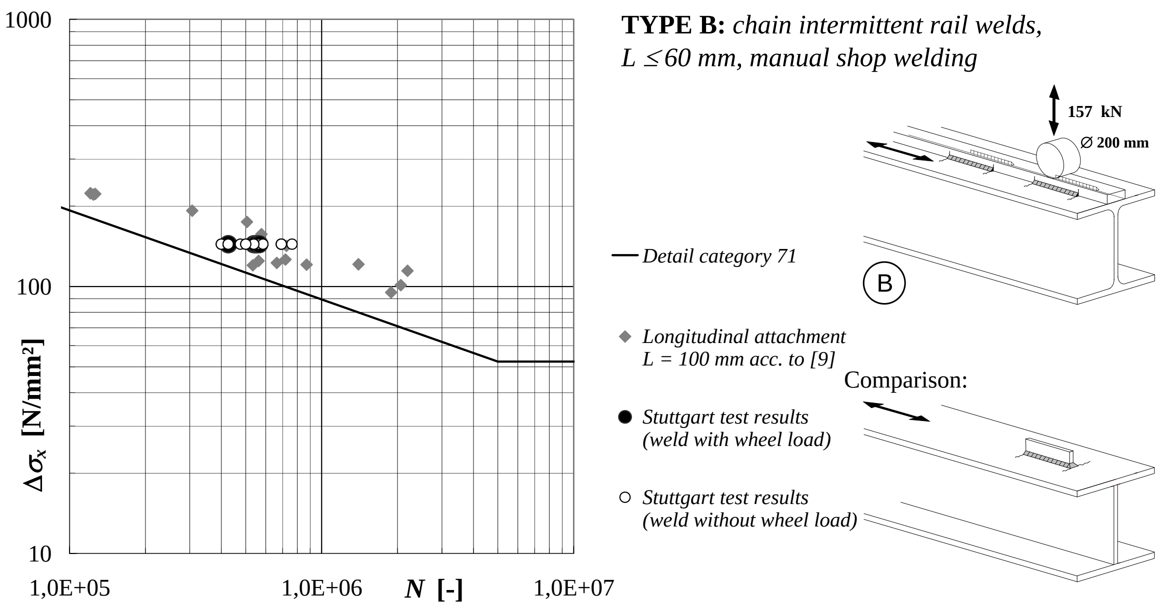

Figure 10. Fatigue strength of chain intermittent rail welds

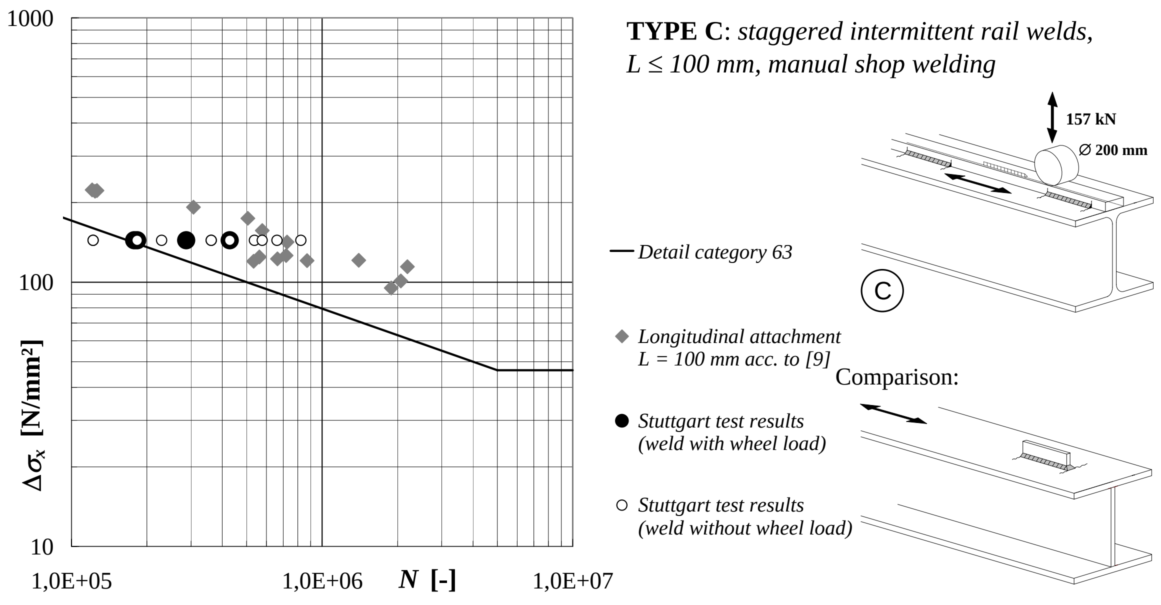

Figure 11. Fatigue strength of staggered intermittent rail welds

5 CONCLUSIONS

In this paper a fatigue verification approach has been presented that allows for taking into account the influence of the multiaxial state of stress due to the wheel load application on the rail welds. This approach does not try to determine the damage contribution of the wheel load directly by a damage accumulation formula but tries to assess the damage contribution by identifying the decrease of the fatigue resistance of the longitudinal fillet welds if an additional wheel load is applied.

For eight test girders the fatigue strengths of the rail welds in tension (longitudinal fillet weld) under additional crane-wheel load induced transverse pressure were determined. Different types of fillet welds were investigated. By using the described approach the fatigue verification can be limited to the assessment of longitudinal stress ranges. However the fatigue strength of the well-known longitudinal fillet weld in tension has to be modified depending on the magnitude of the additionally acting wheel load.

The determined fatigue strengths of continuous rail welds under wheel loading are reduced compared to the fatigue resistance of a longitudinal fillet weld without wheel load. Nevertheless the reduced fatigue strength seems to be at least fatigue category 71.

For intermittent rail welds the notch at the weld ends dominates. The fatigue strengths of the investigated test girders with chain intermittent rail welds were not lower than the fatigue strength of the longitudinal stiffener with $50 < L \leq 80$ mm.

Compared with the chain intermittent ones the staggered intermittent rail welds behave more unfavourably under wheel loading. Nevertheless the determined fatigue strengths of the investigated test girders with staggered intermittent rail welds in general were not lower than the fatigue strength of the longitudinal stiffener with $80 < L \leq 100$ mm.

Up to now the small number of test results has not allowed to formulate statistically confirmed statements. Even so the shown tendencies are quite positive. That is why the longterm goal should be to establish an own-standing fatigue detail in Eurocode 3 Part 1-9 based on a more extensive test series.

The aspect of damage spread throughout the rail and the influence of a non-proportional stressing could not be simulated by means of the research project's test setup. The simulated wheel load could only act stationary on the test girders. Only a test setup including a moving constant wheel load allows for a time-space shift of the loading point. So it has been unrevealed up to now how far the surrounding undamaged material in proximity of the region damaged by the concentrated load develops a beneficial effect.

ACKNOWLEDGEMENT

The work reported in the paper was financed by Arbeitsgemeinschaft industrieller Forschungsvereinigungen "Otto von Guericke" (AiF) and Deutscher Ausschuss fuer Stahlbau (DASt). Special thanks are due to a number of individuals and firms who offered support and encouragement, including Dr.-Ing. H.-P. Guenther and Dipl.-Ing. Chr. Rasche at University Stuttgart, Dr.-Ing. D. Lotze at MPA Stuttgart, Firma Abus in Gummersbach and Firma Goldbeck, Bielefeld.

6 REFERENCES

1. W. Dittrich and L. Ernst, *Hebezeuge und Foerdermittel*, No. 13 , 1973, 205-211
2. K. Wolfram, Zum Einfluss von Druckspannungen auf die Ermuedungsfestigkeit von Stahlbauteilen. Dissertation, TU Dresden, 2001.
3. U. Kuhlmann and M. Euler, Kranbahntraeger - Wirtschaftliche Bemessung und Konstruktion robuster Radlasteinleitungen, final report of AiF / DASt-research project No. 14173, 2007.
4. T. R. Gurney, Fatigue of welded structures, Cambridge University Press, 2nd Edition, Cambridge, 1979, 172-175
5. A. G. Senior and T. R. Gurney, *The Structural Engineer*, Vol. 41 No. 10, 1963, 301-312
6. Eurocode 3 - Design of steel structures - Part 6: Crane supporting structures, February 2007
7. Eurocode 3 - Design of steel structures - Part 1-9: Fatigue, May 2005
8. DIN 4132:1981-02. Kranbahnen Stahltragwerke: Grundsaetze fuer Berechnung, bauliche Durchbildung und Ausfuehrung, German specification, 1981.
9. G. Sedlacek et al. Background Document to prEN 1993-1-9. 1st Draft, October 2004